

Vortex quantum creation and winding number scaling in a quenched spinor Bose gas

Michael Uhlmann¹, Ralf Schützhold^{1,*}, and Uwe R. Fischer^{2,†}

¹*Institut für Theoretische Physik, Technische Universität Dresden, D-01062 Dresden, Germany*

²*Eberhard-Karls-Universität Tübingen, Institut für Theoretische Physik*

Auf der Morgenstelle 14, D-72076 Tübingen, Germany

Motivated by a recent experiment, we study non-equilibrium quantum phenomena taking place in the quench of a spinor Bose-Einstein condensate through the zero-temperature phase transition separating the paramagnetic and ferromagnetic phases. We derive the typical spin domain structure (correlations of the effective magnetization) created by the quench arising due to spin-mode fluctuations, and establish a sample-size scaling law for the creation of spin vortices, which are topological defects in the transverse magnetization.

When a quantum system is driven far away from its equilibrium state, many-body effects may occur in a distinctly non-classical way [1, 2]. The tightly controlled study of such phenomena became possible because of the rapid experimental progress made with dilute atomic gases. Due to their rarefied state, the timescales on which the equilibrium state is restored become long compared to typical response times of dense systems (like superfluid helium), so that out-of-equilibrium phenomena become accessible within the typical time span of an experiment.

Spinor Bose-Einstein condensates are created by trapping different hyperfine states of a particular atomic species by optical means [3], which enables, *inter alia*, the investigation of coherent spin-exchange dynamics [4], and the formation of spin domains by a dynamical instability [5]. Genuine non-equilibrium quantum effects in a spinor Bose gas were realized in a recent experiment [6], where an initially paramagnetic state was rapidly quenched through a quantum phase transition to a final ferromagnetic state. Such a quench results in spin vortices (imaged *in situ* by phase contrast techniques [7]), which are topological defects in the magnetization with a paramagnetic core [8, 9]. The creation of such defects is founded on the Kibble-Zurek mechanism [10, 11] and its quantum version [12], which explains their creation in a second-order symmetry-breaking phase transition. An important difference of the experimentally realized Bose-Einstein condensates to a conventional condensed matter system, to be taken into account when calculating how many topological defects are created in a quench, is that total angular momentum is always exactly conserved. A uniform, conventional “ferromagnetic” net magnetization of the gas sample from an initially unpolarized state is therefore prohibited, and a complicated spin domain structure generally develops.

In what follows, we derive the spectrum of fluctuations induced by a rapid quench to the ferromagnetic state of a spinor Bose gas, and establish a general sample-size dependent scaling law for the resulting variance of the net number of spin vortices. Besides the total defect density, the typical excess number of vortices within a given area determines the spectrum of the created magneti-

zation fluctuations. Both quantities have implications, *inter alia*, for the scattering of quasi-particles (e.g., ferromagnetic magnons) at the defects, affecting measurable transport properties like conductivity and susceptibility. Therefore, spinor Bose gases (apart from being interesting in their own right) serve as a useful and experimentally accessible toy model for the general case.

The dilute spinor Bose gas can be described in terms of multi-component field operators $\hat{\psi}_a$ whose dynamics is governed by the Hamiltonian density ($\hbar = 1$)

$$\hat{\mathcal{H}} = \frac{1}{2m}(\nabla\hat{\psi}_a^\dagger) \cdot \nabla\hat{\psi}_a + V_{\text{trap}}\hat{\psi}_a^\dagger\hat{\psi}_a + \frac{c_0}{2}\hat{\psi}_a^\dagger\hat{\psi}_b^\dagger\hat{\psi}_b\hat{\psi}_a + \frac{c_2}{2}\mathbf{F}_{ab} \cdot \mathbf{F}_{cd}\hat{\psi}_a^\dagger\hat{\psi}_c^\dagger\hat{\psi}_b\hat{\psi}_d - q\hat{\psi}_z^\dagger\hat{\psi}_z, \quad (1)$$

where m denotes the mass of the atoms. The vector \mathbf{F}_{ab} contains the spin matrices [13] and determines the effective magnetization $\hat{\mathbf{F}} = \mathbf{F}_{ab}\hat{\psi}_a^\dagger\hat{\psi}_b/\varrho$, where a summation over component indices a, b, c, d is implied and $\varrho = \langle\hat{\psi}_a^\dagger\hat{\psi}_a\rangle$ is the total (conserved) density. For spin-one systems, the sum runs over $a = 0, \pm 1$ or, alternatively, over $a = x, y, z$ with $\psi_0 = \psi_z$ and $\psi_\pm = (\psi_x \pm i\psi_y)/\sqrt{2}$. The coupling constants $c_0 = 4\pi(a_0 + 2a_2)/(3m)$ and $c_2 = 4\pi(a_2 - a_0)/(3m)$ are determined by scattering lengths a_S for the scattering channel with total spin S . For $c_0 \gg |c_2|$, density fluctuations are energetically suppressed in comparison with the spin modes. Furthermore, the relevant wavelengths are assumed to be much smaller than the system size, allowing for a quasi-homogeneous description, so that we may omit the scalar trapping potential V_{trap} and approximate $\varrho = \text{const}$. Finally, q denotes the strength of the quadratic (one-particle) Zeeman shift qF_z^2 [6], where an external magnetic field is oriented along the z direction (the linear Zeeman shift can be omitted, because the Larmor precession frequency is much larger than all other frequency scales [8]).

Assuming $c_2 < 0$, the system is ferromagnetic for vanishing Zeeman shift $q = 0$, i.e., the magnetization $\hat{\mathbf{F}}$ assumes a maximum value $\langle\hat{\mathbf{F}}\rangle^2 = 1$ in some given but arbitrary direction (broken-symmetry phase). For small but non-zero q , the magnetization $\langle\hat{\mathbf{F}}\rangle$ lies in the x, y -plane due to the term qF_z^2 but is still maximal, $\langle\hat{\mathbf{F}}\rangle^2 = 1$. For large q , however, the ground state corresponds to a

condensate in the $\psi_0 = \psi_z$ component only and the symmetry is restored, i.e., the magnetization $\langle \hat{\mathbf{F}} \rangle$ vanishes (paramagnetic phase). Hence, by rapidly lowering q , we may quench the system from an initially paramagnetic to an (effectively two-dimensional) ferromagnetic phase.

In order to study the evolution of the quantum field during the quench, we employ a number-conserving mean-field ansatz [14] $\hat{\psi}_z = (\psi_{\text{co}} + \delta\hat{\psi}_z)\hat{A}/\sqrt{\hat{N}}$, which is adapted to the initial paramagnetic phase but can be extrapolated for some finite time after the quench [15]. This ansatz allows for a linearized expression for the magnetization (which assumes in Cartesian coordinates the simple form $\hat{F}_a = -i\varepsilon_{abc}\hat{\psi}_b^\dagger\hat{\psi}_c/\varrho$) and to derive an effective mean-field Hamiltonian for transverse magnetization $\hat{\mathbf{F}}$ from the full Hamiltonian Eq. (1),

$$\frac{\hat{\mathcal{H}}_{\text{eff}}}{\varrho} = \frac{\hat{\mathbf{\Pi}}}{\varrho} \left(q - \frac{\nabla^2}{2m} \right) \frac{\hat{\mathbf{\Pi}}}{\varrho} + \hat{\mathbf{F}} \left(\frac{q + 2c_2\varrho}{4} - \frac{\nabla^2}{8m} \right) \hat{\mathbf{F}}, \quad (2)$$

with $\hat{\mathbf{\Pi}} = (\psi_{\text{co}}\hat{\psi}_y^\dagger + \psi_{\text{co}}^*\hat{\psi}_y, -\psi_{\text{co}}\hat{\psi}_x^\dagger - \psi_{\text{co}}^*\hat{\psi}_x)/2$, being the canonical momentum operator for spin-one bosons. The experiment [6] is described by a two-dimensional transverse magnetization $\hat{\mathbf{F}} = (\hat{F}_x, \hat{F}_y)$ obeying the $SO(2)$ -symmetry of rotations around the z -axis in effectively two spatial dimensions $\nabla = (\partial_x, \partial_y)$, permitting topological defects in the form of spin vortices. However, the above expressions for the Hamiltonian are completely analogous for a $SO(N)$ -symmetry of the order parameter $\langle \hat{\mathbf{F}} \rangle$ in $N > 2$ spatial dimensions, where the analogous topological defects are generically called “hedgehogs”, see, e.g., [16, 17, 18, 19]. Therefore, we shall discuss the general $SO(N)$ situation in the following and return to the experimentally realized example $N = 2$ of [6] at the end.

The simple expression (2) allows us to directly read off the critical value $q_{\text{cr}} = 2|c_2|\varrho$ of the phase transition. After a quench from $q_{\text{in}} > q_{\text{cr}}$ to $q_{\text{out}} < q_{\text{cr}}$, and using a normal-mode expansion, we obtain exponentially growing modes corresponding to imaginary frequencies $\omega_k^q = \sqrt{(\epsilon_k + q)(\epsilon_k + q + 2c_2\varrho_0)}$, where $\epsilon_k = k^2/(2m)$, cf. Fig. 1. There are two regimes: For $q_{\text{cr}} > q_{\text{out}} > q_{\text{cr}}/2$, the exponential growth rate $\Im(\omega_k^q)$ of the normal modes increases with their wavelength, but for $q_{\text{out}} < q_{\text{cr}}/2$, the growth rate assumes its maximum at a given wavenumber $k_{\text{max}} = \sqrt{m(q_{\text{cr}} - 2q_{\text{out}})}$. In view of the experimental parameters [6], we shall focus on the second scenario. Assuming the Bose gas to be sufficiently dilute, we may extrapolate our linearized (mean-field) description (2) to intermediate times t which contain many e -foldings $\Im(\omega_{k_{\text{max}}}^q)t \gg 1$ of the exponentially growing modes [15], whereas the magnetization is still small enough, $\mathbf{F}^2 \ll 1$, to be in the linear regime. In this limit, expectation values containing the magnetization are dominated by the fastest-growing modes with $|\mathbf{k}| = k_{\text{max}}$, and thus can be calculated by approximating the $d^N k$ -integrals via the saddle-point method. Since the initial state (paramagnetic phase) is supposed to be globally isotropic such as

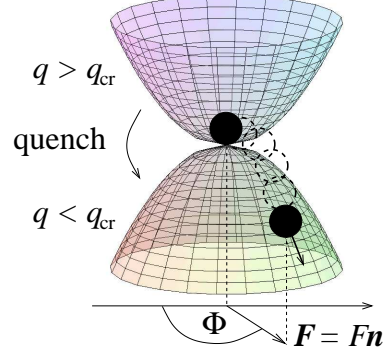


FIG. 1: Inversion behaviour of the effective potential from (2). After crossing the critical point, the direction \mathbf{n} of the effective magnetization \mathbf{F} in the plane, at any given point in space, gets frozen at a particular angle Φ , while its modulus F continues to grow exponentially in time (“rolls down” the potential hill).

the thermal ensemble or the ground state of (2), the dominant contribution to the two-point magnetization correlation function is calculated to be

$$\langle \hat{F}_a(\mathbf{r})\hat{F}_b(\mathbf{r}') \rangle = C_{\nu}^{\text{max}} \delta_{ab} \frac{\exp\{q_{\text{cr}}t\}}{\sqrt{t}} \frac{J_{\nu}(k_{\text{max}}|\mathbf{r} - \mathbf{r}'|)}{(k_{\text{max}}|\mathbf{r} - \mathbf{r}'|)^{\nu}}, \quad (3)$$

where J_{ν} is the Bessel function of the first kind with the index $\nu = N/2 - 1$. The coefficient C_{ν}^{max} depends on k_{max} , ν , q_{out} , sweep rate, and temperature etc., i.e., all information about the initial state (as long as it is isotropic) enters this pre-factor only.

Now let us study the creation of topological defects, i.e., $SO(N)$ -hedgehogs, by the symmetry-breaking quench. Their characteristic size, i.e., the extent of the paramagnetic core, can be determined by comparing the kinetic term $\propto \nabla^2$ with the c_2 -contribution in (1) which yields $\xi = 1/\sqrt{2|c_2|\varrho m} = 1/\sqrt{m\bar{q}_{\text{cr}}}$, i.e., the spin healing length. In order to deal with well-separated and therefore well-defined topological defects, we assume that the dominant wave-length $\lambda_{\text{max}} = 2\pi/k_{\text{max}}$ (determining their typical distance, see below) is much larger than the spin healing length ξ , which amounts to requiring $0 < q_{\text{cr}} - 2q_{\text{out}} \ll q_{\text{cr}}$. This condition is reasonably well satisfied in the experiment [6] where $\xi \approx 2.4 \mu\text{m}$ and $\lambda_{\text{max}} \approx 16 \mu\text{m}$.

Therefore, within the saddle-point approximation (i.e., focusing on the dominant modes), the term $-\nabla^2 \rightarrow k_{\text{max}}^2$ in the equations of motion resulting from (2) can be neglected compared to q_{cr} and we may approximate $\hat{\mathbf{F}} \approx q_{\text{cr}}^2 \mathbf{F}/4$. Consequently, at each spatial position, the magnetization \mathbf{F} behaves as the coordinate of a harmonic oscillator (in N dimensions), becoming inverted upon crossing the transition, cf. Fig. 1. Splitting \mathbf{F} up into its modulus F and unit vector of direction \mathbf{n} via $\mathbf{F} = Fn$, we find that F grows exponentially whereas the dynamics of \mathbf{n} freezes: In view of the conserved “angular momentum”

$\mathbf{L} = \mathbf{F} \times \dot{\mathbf{F}}$, we find that $|\dot{\mathbf{n}}| = |\mathbf{L}|/F^2 \propto F_0^2/F^2(t)$ decreases rapidly. Ergo, after a short time (of order $1/q_{\text{cr}}$), the magnetization \mathbf{F} at each spatial position \mathbf{r} grows exponentially in some given direction $\mathbf{n}(\mathbf{r})$, i.e., the system rolls down the parabolic potential hill whereby the direction of descent does not change anymore, cf. Fig. 1. The correlations between the frozen directions \mathbf{n} at different spatial positions are governed by the initial state and determine the seeds for the creation of topological defects – i.e., objects which cannot be deformed to a constant \mathbf{n} in a smooth way [17].

The topological defects we are considering are $SO(N)$ (anti-)hedgehogs in N spatial dimensions with the typical order parameter distribution $\mathbf{n} = \pm \mathbf{r}/r$ and can be characterized by a non-vanishing winding number, i.e., a topological invariant belonging to the homotopy group $\pi_{N-1}(S_{N-1}) = \mathbb{Z}$. The winding number is calculated by an integral over a $N-1$ -dimensional hypersurface enclosing a N -dimensional volume [18]:

$$\hat{\mathfrak{N}} = \oint dS_\alpha \frac{\varepsilon_{abc\dots} \varepsilon^{\alpha\beta\gamma\dots}}{\Gamma(N) \mathcal{S}_{N-1}} \hat{n}^a (\partial_\beta \hat{n}^b) (\partial_\gamma \hat{n}^c) \dots \quad (4)$$

Here $\mathcal{S}_{N-1} = 2\pi^{N/2}/\Gamma(N/2)$ denotes the surface of the unit sphere embedded in N dimensions, and ε are the N -dimensional Levi-Civita symbols. Since the winding number counts the difference between hedgehogs and anti-hedgehogs, its expectation value vanishes, $\langle \hat{\mathfrak{N}} \rangle = 0$ (conservation of magnetization), but its variance $\langle \hat{\mathfrak{N}}^2 \rangle$ as a function of the enclosed volume yields the desired spectrum of net magnetization fluctuations.

In order to calculate $\langle \hat{\mathfrak{N}}^2 \rangle$, we make an additional approximation: For a N -dimensional harmonic oscillator $\hat{\mathbf{F}} \approx q_{\text{cr}}^2 \mathbf{F}/4$, the ground-state probability distribution $p(F) \propto F^{N-1} \exp\{-F^2\}$ of the amplitude F is peaked around a (for $N > 1$) non-zero value and the relative width of this peak decreases with increasing N , e.g., $\langle \hat{F}^4 \rangle / \langle \hat{F}^2 \rangle^2 - 1 \propto 1/N$. Therefore, we approximate the operator \hat{F} by an exponentially growing classical value $\hat{F} \rightarrow F(t)$ in all expectation values. This semiclassical approximation will become asymptotically exact in the limit $N \uparrow \infty$, but we expect it to yield qualitatively correct results also in lower dimensions down to $N = 2$ since $p(F)$ is discernibly peaked even for $N = 2$ and the topological defects are mainly determined by the (quantum) fluctuations of $\hat{\mathbf{n}}$ (and not of \hat{F}). Note that all the linearized \hat{F}_a possess independent initial ground states and commute with each other. Therefore, the \hat{n}_a do also commute with each other [so that operator ordering in (4) is not an issue] and with \hat{F} , which ultimately makes possible the semiclassical approximation of $\hat{F} \rightarrow F$.

The above approach enables us to calculate $\langle \hat{\mathfrak{N}}^2 \rangle$ in arbitrary dimensions $N \geq 2$. After inserting (4) and using the semiclassical approximation $\hat{F}(t, \mathbf{r}) \approx F(t) \hat{\mathbf{n}}(\mathbf{r})$, the expectation value can be decomposed into a product of N two-point correlators (3). Let us exemplify this proce-

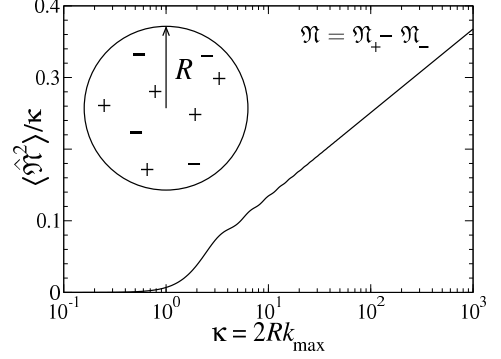


FIG. 2: Scaling of the variance of the winding number $\langle \hat{\mathfrak{N}}^2 \rangle$ with the sample size R . A logarithmic plot of $\langle \hat{\mathfrak{N}}^2 \rangle / \kappa$ is used in order to visualise the cross-over from κ^4 to $\kappa \ln \kappa$ scaling.

dure for two spatial dimensions: The transverse magnetization can be decomposed via $\hat{F}_\perp = \hat{F}_x + i\hat{F}_y = \hat{F}e^{i\hat{\Phi}}$ into its modulus \hat{F} and phase $\hat{\Phi}$ which commute and are both self-adjoint [20]. The winding number (4) reads [21]

$$\hat{\mathfrak{N}} = \frac{1}{2\pi} \oint_{\mathcal{C}} dl \cdot \nabla \hat{\Phi} = \oint_{\mathcal{C}} dl \cdot \frac{\hat{F}_x \nabla \hat{F}_y - \hat{F}_y \nabla \hat{F}_x}{2\pi \hat{F}^2}. \quad (5)$$

Using Eq. (3), replacing $\hat{F} \rightarrow F$, and choosing the contour \mathcal{C} as a circle with radius R , we get

$$\langle \hat{\mathfrak{N}}^2(R) \rangle = \frac{\kappa^2}{2\pi} \int_0^1 dx \sqrt{1-x^2} J_1^2(\kappa x), \quad (6)$$

with $\kappa = 2Rk_{\text{max}}$, cf. Fig. 2. As anticipated, the characteristic length scale (e.g., typical distance between vortices) is set by the dominant wavelength λ_{max} (instead of the spin healing length ξ , for example).

For small κ , we Taylor-expand the Bessel function in Eq. (6), $J_1(\kappa x) = \kappa x/2 + \mathcal{O}[(\kappa x)^3]$, and obtain (cf. Fig. 2)

$$\langle \hat{\mathfrak{N}}^2(\kappa \ll 1) \rangle = \frac{\kappa^4}{128} + \mathcal{O}[\kappa^5]. \quad (7)$$

Interestingly, the probability of finding a vortex inside a circle with area πR^2 (cf. Fig. 2) scales as R^4 instead of R^2 . Note that this scaling behaviour is valid for $R \ll \lambda_{\text{max}}$, but R can still be much larger than ξ , i.e., the scaling behaviour is not an effect of the finite vortex core size. This finding invalidates the naive classical picture of independent and random vortices (which would imply an R^2 scaling). Instead the winding numbers of neighbouring circles are anti-correlated and not independent. This non-classical scaling persists in higher dimensions: The variance of the winding number in a small volume R^N scales as R^{2N} instead of R^N (as in the classical picture).

Another interesting limit is the large-scale spectrum of the winding number, i.e., the difference between the

number of vortices and anti-vortices $\mathfrak{N} = \mathfrak{N}_+ - \mathfrak{N}_-$. Typically, two popular models for scaling behaviour are discussed in the literature [11, 16]. Assuming a random distribution of vortices and anti-vortices (*random vortex gas* model), the typical difference $|\mathfrak{N}|$ scales with $\sqrt{\mathfrak{N}_\pm}$. Because the total number $\mathfrak{N}_+ + \mathfrak{N}_-$ increases proportional to the area R^2 , this model predicts a scaling of $\langle \hat{\mathfrak{N}}^2 \rangle \sim R^2$ ($N = 2$). Alternatively, the *random phase walk* model assumes a random walk of the phase Φ along the circumference of the circle. The accumulated winding number $|\mathfrak{N}|$ scales with \sqrt{R} in this situation, implying a scaling of $\langle \hat{\mathfrak{N}}^2 \rangle \sim R$. Of course, both models cannot be the final truth (consider the deformation of the circle to a slim ellipse, for example), and it is not obvious how to generalize the random phase walk model to higher dimensions – but one can compare the different predictions with our approach. For large κ , the asymptotic expansion $J_1(\kappa x \uparrow \infty) \propto \cos(\kappa x - 3\pi/4)/\sqrt{\kappa x}$ yields (cf. Fig. 2)

$$\langle \hat{\mathfrak{N}}^2(\kappa \gg 1) \rangle \sim \kappa \ln \kappa, \quad (8)$$

which is close to the scaling predicted by the random phase walk model – but still not quite in agreement due to the additional factor of $\ln \kappa$. [This extra factor arises from the slow decay of the two-point correlator (3) at large distances $|\mathbf{r} - \mathbf{r}'|^{-1/2}$ and is thus only valid within the saddle-point approximation, i.e., for large times t .]

Finally, let us study intermediate κ values: In Ref. [22], the defect density is calculated to be $k_{\max}^2/(4\pi)$ treating the magnetization as a Gaussian stochastic field. Hence, a circle with a radius of $R = 2/k_{\max}$ should typically contain one (anti-)vortex. However, if we calculate $\langle \hat{\mathfrak{N}}^2 \rangle$ at $\kappa = 4$, we obtain around $1/3$ instead of one. Although the discrepancy is not huge, it already suggests that our results are not quite compatible with Ref. [22], and thus experiment should judge which approach yields the better description. Alternatively, numerical simulations (supplemented by suitable assumptions about the initial noise spectrum) provide a complementary approach [23].

In conclusion, for the example of a spinor Bose gas, we studied the creation of topological defects during the quench from the paramagnetic to the $SO(N)$ -symmetry breaking ferromagnetic phase. By means of the extrapolation of a mean-field ansatz [24], we found that the direction \mathbf{n} of the effective magnetization \mathbf{F} freezes during the quench while its magnitude F grows exponentially. Hence, we were able to derive the (frozen) winding number $\hat{\mathfrak{N}}$ of the seeds for $SO(N)$ topological defects and to predict its scaling behaviour, which is universal in the sense that it does not depend on temperature and sweep rate etc., as long as the initial state is globally isotropic.

R. S. and M. U. acknowledge support by the Emmy Noether Programme of the German Research Foundation (DFG) under grant No. SCHU 1557/1-2. We thank D. M. Stamper-Kurn and G. E. Volovik for valuable discussions and acknowledge support by ESF-COSLAB.

* schuetz@theory.phy.tu-dresden.de † uwe.fischer@uni-tuebingen.de

- [1] T. Kinoshita, T. Wenger, and D. S. Weiss, *Nature* **440**, 900 (2006).
- [2] A. K. Tuchman, C. Orzel, A. Polkovnikov, and M. A. Kasevich, *Phys. Rev. A* **74**, 051601(R) (2006); W. Li, A. K. Tuchman, H.-C. Chien, and M. A. Kasevich, preprint quant-ph/0609009, to appear in *Phys. Rev. Lett.*
- [3] J. Stenger *et al.*, *Nature* **396**, 345 (1998).
- [4] M.-S. Chang, Q. Qin, W. Zhang, L. You, and M. S. Chapman, *Nature Phys.* **1**, 111 (2005).
- [5] W. Zhang, D. L. Zhou, M.-S. Chang, M. S. Chapman, and L. You, *Phys. Rev. Lett.* **95**, 180403 (2005).
- [6] L. E. Sadler, J. M. Higbie, S. R. Leslie, M. Vengalattore, and D. M. Stamper-Kurn, *Nature* **443**, 312 (2006).
- [7] J. M. Higbie *et al.*, *Phys. Rev. Lett.* **95**, 050401 (2005).
- [8] H. Saito and M. Ueda, *Phys. Rev. A* **72**, 023610 (2005).
- [9] H. Saito, Y. Kawaguchi, and M. Ueda, *Phys. Rev. Lett.* **96**, 065302 (2006).
- [10] T. W. B. Kibble, *J. Phys. A* **9**, 1387 (1976); W. H. Zurek, *Nature* **317**, 505 (1985).
- [11] M. Hindmarsh and T. W. B. Kibble, *Rep. Prog. Phys.* **58**, 477 (1995); W. H. Zurek, *Phys. Rep.* **276**, 177 (1996).
- [12] W. H. Zurek, U. Dorner, and P. Zoller, *Phys. Rev. Lett.* **95**, 105701 (2005).
- [13] T. Ohmi and K. Machida, *J. Phys. Soc. Jpn.* **67**, 1822 (1998); T.-L. Ho, *Phys. Rev. Lett.* **81**, 742 (1998).
- [14] Here $\hat{N} = \hat{A}^\dagger \hat{A}$ counts the total number of particles, cf. C. W. Gardiner, *Phys. Rev. A* **56**, 1414 (1997); Y. Castin and R. Dum, *Phys. Rev. A* **57**, 3008 (1998).
- [15] R. Schützhold, M. Uhlmann, Y. Xu, and U. R. Fischer, *Phys. Rev. Lett.* **97**, 200601 (2006).
- [16] G. E. Volovik and V. P. Mineev, *Zh. Éksp. Teor. Fiz.* **73**, 767 (1977) [Sov. Phys. JETP **46**, 401 (1977) contains a misprint in Eq. (2.4); in the denominator “6”, i.e., $\Gamma(4)$, was replaced by “8”]; G. E. Volovik, *The Universe in a Helium Droplet* (Oxford University Press, 2003).
- [17] N. D. Mermin, *Rev. Mod. Phys.* **51**, 591-648 (1979); L. Michel, *Rev. Mod. Phys.* **52**, 617-651 (1979).
- [18] A. G. Abanov and P. B. Wiegmann, *Nucl. Phys. B* **570**, 685 (2000).
- [19] C. M. Savage and J. Ruostekoski, *Phys. Rev. A* **68**, 043604 (2003).
- [20] Note that this is distinct from the nonvanishing commutator of density and phase operators resulting from the analogous decomposition of the single-component field operator $\hat{\psi} = \exp[i\hat{\Phi}]\sqrt{\hat{\rho}}$, which underlies the definition of conventional momentum/velocity vortices in a fluid.
- [21] In contrast to spin vortices, domain walls (lines with vanishing F) are not topologically stable for the order parameter considered here. Thus, the domain boundaries observed in [6] are line-like regions with small but not vanishing F , and do not enter Eqs. (4) and (5).
- [22] A. Lamacraft, preprint cond-mat/0611017.
- [23] H. Saito, Y. Kawaguchi, and M. Ueda, preprint cond-mat/0610862.
- [24] Note that our results do only describe the initial stage and are, strictly speaking, only valid in the linear regime, i.e., as long as the directions $\mathbf{n}(\mathbf{r})$ are frozen. The subsequent non-linear dynamics, including annihilations of vortex–anti-vortex pairs etc., is not taken into account.